JOURNAL OF MATERIALS SCIENCE 28 (1993) 4667–4672

Microbuckling instability in elastomeric cellular solids

R. LAKES
Department of Biomedical Engineering, Department of Mechanical Engineering, Center for Laser Science and Engineering, University of Iowa, Iowa City, IA 52242, USA

P. ROSAKIS, A. RUINA
Department of Theoretical and Applied Mechanics, Cornell University, Ithaca, NY 14853, USA

Compressive properties of elastic cellular solids are studied via experiments upon foam and upon single-cell models. Open-cell foam exhibits a monotonic stress–strain relation with a plateau region; deformation is localized in transverse bands. Single-cell models exhibit a force–deformation relation which is not monotonic. In view of recent concepts of the continuum theory of elasticity, the banding instability of the foam in compression is considered to be a consequence of the non-monotonic relation between force and deformation of the single cell.

1. Introduction

Cellular solids are currently used in many structural applications. It is therefore of interest to understand as fully as possible the physical mechanisms for deformation and damage formation. With sufficient understanding it will be possible to develop new cellular solids with superior resistance to damage.

Elastomeric foams are known to exhibit several regions of behaviour in simple uniaxial compression: (i) an approximately linear behaviour for strains less than about 0.05, (ii) a plateau region in which strain increases at constant or nearly constant stress, and (iii) a densification region of the stress–strain curve in which its slope increases markedly with strain. Linear elasticity arises from bending of the cell ribs, the plateau arises from their elastic buckling, and densification arises from contact between ribs [1]. Simple analytical models based on elastic buckling of the ribs have been used in an effort to predict the behaviour of foams. They indicate a value of strain at which the transition between linear elasticity and plateau regions occurs at about 0.05, which corresponds closely with experiment [1].

Ductile foams such as those made of metals also exhibit regions of linear elasticity, plateau, and densification. In ductile foams, the plateau region is associated with plastic buckling of cell ribs rather than elastic buckling. Moreover, in elastomeric foams, rib buckling is fully reversible (though accompanied by hysteresis), in ductile foams, rib buckling is associated with permanent microdamage.

The purpose of this paper is to advance understanding of compressive collapse in cellular solids with the aid of the theory of stability of elastic continua. Since elastomeric foams are more representative of elastic continua than ductile foams, consideration is given to rib microbuckling of elastomeric foams and its relation to elastic-stability considerations of the foam as a whole. Ductile foams, which are more important in applications requiring the support of relatively large stresses, will be considered in a later study.

2. Materials and methods

Scott Industrial Foam, which is a reticulated, open-cell polyurethane foam, was examined experimentally to determine its mechanical properties. The pore size was 1.3 mm (20 pores per inch). Macroscopic models of individual cells were also prepared from rods of polyurethane rubber, 6.1 mm in diameter. Open-cell models in the shape of a tetrakaidecahedron (with ribs 25 mm long) and a regular octahedron (with ribs 50 mm long) were made. The tetrakaidecahedron has six square faces and eight regular hexagonal faces (Fig. 1); it is considered representative of typical cells in foams.

Mechanical testing was conducted using a servohydraulic testing machine (Instron, Canton, MA, model 1321) at room temperature (22 °C, 55% relative humidity). The specimens were mounted between rigid platens and held by friction in compression tests. Some tests of compression and tension were done with the specimen cemented to the platens with cyanoacrylate adhesive. Several trials were also conducted in which compression specimens were lubricated with a silicone-spray lubricant. Long blocks of foam in compression tests were restrained laterally on one or two surfaces to prevent macroscopic buckling. Some torsion tests were made upon square-cross-section bars as well; however, the interpretation of such tests is less simple than for compression as a result of the inhomogeneous strain field in torsion of a bar. The foam was examined visually and under low-power magnification during deformation. The tetrakaidecahedron

0022–2461

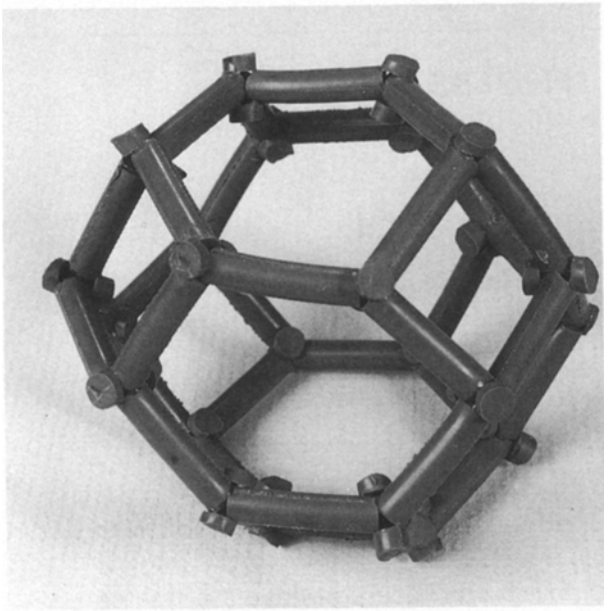

Figure 1 Tetrakaidecahedron cell model.

model was loaded in compression upon a pair of square faces and a pair of hexagonal faces in separate tests. The octahedron model was loaded upon a pair of triangular faces and a pair of vertices in separate tests. Triangular waveforms at slow deformation rates (0.033 to 0.0033 cycle sec^{-1}) in displacement control were used. The strains presented in the graphs were calculated from the platen-displacement signal.

3. Experimental results

Uniaxial compression of blocks of Scott Industrial Foam of different size and shape resulted in the stress–strain curves shown in Fig. 2. Observe that the curves are monotonic. The results for a large block longer than its width agree with those of Choi and Lakes [2]. Further experiments upon compression specimens which were lubricated or cemented to the platens disclosed similar behaviour. The overall shape of the curves was insensitive to changes in strain rate. A small block, also longer than its width behaved similarly to the large block, as shown in Fig. 2.

Bands of localized deformation were observed visually, and they were transverse to the direction of compression. The bands contained cells which were highly compressed to the point of contact between adjacent ribs. The bands were of low contrast. The bands began to form when the gauge length of the specimen reached a strain of about 0.1, and they were very evident at a strain of 0.2. Further compression within the plateau region of strain resulted in an increase in the number of bands, until they occupied most of the specimen; macroscopic densification then occurred. The band thickness depended on the cell size; the bands were several cells thick in foam of cell size 0.4 mm and in foam of cell size 1.2 mm. Banding localization is known to occur in the tensile loading of polymers and metals beyond the yield point, and in plastic deformation of ductile honeycombs [3]. In the case of the present polymer foam, the banding localization was completely reversible, i.e. the bands disappeared upon the removal of the load.

The foams exhibited considerable hysteresis, both in loading from zero into the densification region and in loading over a restricted range of deformation. In the latter case, a measure, Δ, of hysteresis loss was defined as the ratio of the hysteresis-loop width in load to the total excursion in load. In linear viscoelasticity the hysteresis-loop is elliptical and the above ratio is $\sin\delta$ in which δ is the loss angle. For strain excursions of 0.09 peak-to-peak, $\Delta = 0.11$ for excursions about zero,

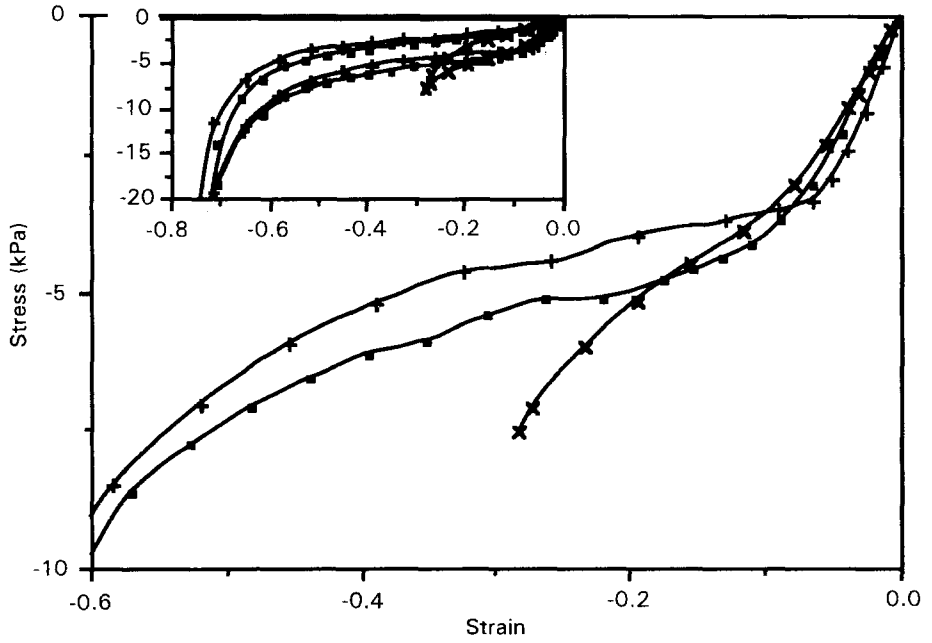

Figure 2 Experimental engineering stress versus engineering strain for monotonic loading in compression for Scott Industrial Foam (20 pore $inch^{-1}$): (■) a block 52 by 53 by 121 mm long, (+) a block 15 by 15 by 19 mm long, and (×) a stubby block 52 by 53 by 19 mm long. The inset shows the stress–strain curves on a wider strain scale and includes hysteresis during loading and unloading; the same symbols are used as in the large graph.

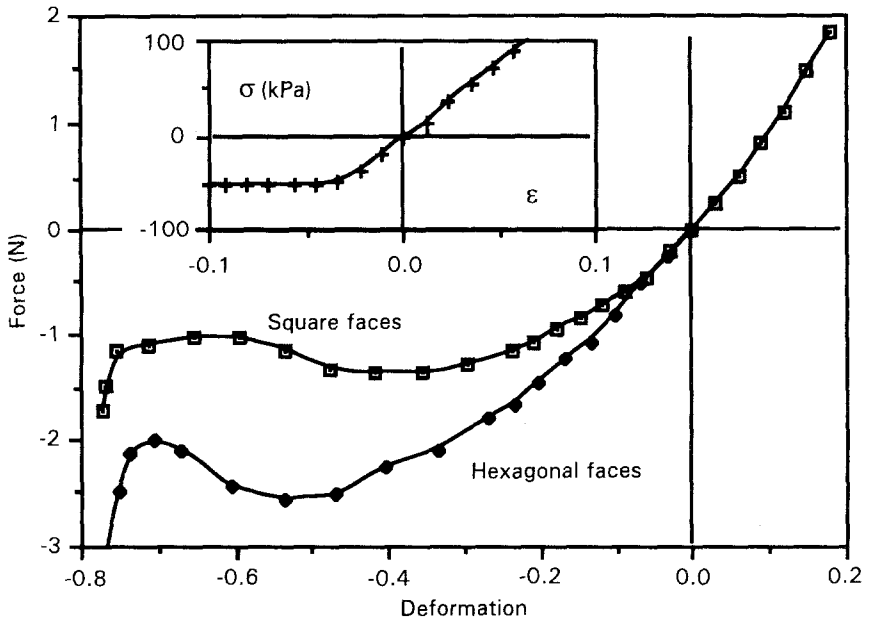

Figure 3 Experimental axial force versus deformation (calculated as the change in cell width divided by the original cell width) for a tetrakaidecahedral cell model with ribs 25 mm long and 6 mm in diameter. The inset shows an engineering stress versus strain ($\Delta L/L$) curve for a single rib. The plateau in compression corresponds to buckling and postbuckling.

$\Delta = 0.24$ in the plateau region ($\varepsilon = 0.2$ to 0.43), and $\Delta = 0.19$ in the densification region ($\varepsilon = 0.73$).

The compressive behaviour of a stubby block, shorter in the load direction than its width, differed from the above in that there was essentially no plateau region, as shown in Fig. 2. The behaviour of a thin layer of foam, about two cells thick, cemented to rigid platens was similar to that of the stubby block.

The compressive behaviour of the tetrakaidecahedron cell model was *not* monotonic, as shown in Fig. 3, in contrast to the behaviour of the foam as a whole. The load–deformation curve displayed a *negative slope* over a range of strain; outside this range the slope was positive. The curve had this shape regardless of whether the compression load was applied to the square faces or to the hexagonal faces. An octahedron cell model also exhibited a non-monotonic load–deformation curve of similar shape to the above. The tetrakaidecahedron-single-cell model behaved similarly to the foam in that the region of approximately linear behaviour was of similar extent; densification began to occur at about the same strain, and rib alignment in tension caused a similar nonlinearity. The principal difference is the presence or failure of monotonicity in the plateau region. During compression, the tetrakaidecahedron cell model first bulged outward in the transverse directions, then assumed a biconcave shape, then the ribs came in contact resulting in a rapid increase in stress.

Torsion tests upon a square-cross-section-foam specimen disclosed load–deformation curves with slopes which varied smoothly by a small amount. There were no abrupt changes in slope nor were there plateau regions. Torsion of a specimen under precompression of 24% or tension of 37% axial strain had no dramatic effect on the shape of the load–deformation curve. No localization in the form of bands was observed in any torsion test.

As for foam materials with negative Poisson's ratios [4, 5], prior study disclosed the absence of a plateau region in the stress–strain curves. In the present study compressed specimens were examined for a banding instability, but none was found.

4. Considerations of stability in elastic continua

The experimental observation of band formation in the compression of foams is considered to be a manifestation of elastic instability. To aid in the interpretation of the results, salient aspects of the theory of stability in elastic continua are presented.

4.1. Linear elasticity

There are several ranges of elastic constants which are associated with stability on various levels. Consider first the case of linear isotropic elasticity. The strain energy is positive definite if and only if the shear modulus, G, and Poisson's ratio, ν, satisfy

$$G > 0, \qquad -1 < \nu < 0.5 \tag{1}$$

or equivalently, $G > 0$ and $3\lambda + 2G > 0$ in which λ and G are the Lamé constants.

Materials which obey these relations give rise to unique solutions of boundary-value problems in which either surface traction or surface displacements are specified. Moreover, such materials are stable to small macroscopic perturbations.

Displacement-type boundary-value problems have unique solutions if [6]

$$G > 0, \qquad -\infty < \nu < 0.5 \text{ and } 1 < \nu < \infty \tag{2}$$

This range is considerably less restrictive than Equation 1. Moreover, other ranges for uniqueness can be obtained for specific boundary shapes.

The conditions for strong ellipticity are [7]

$$G > 0, \qquad \lambda + 2G > 0 \tag{3}$$

If strong ellipticity is violated, the material may exhibit an instability associated with the formation of bands of inhomogeneous deformation [7]. The physical significance of the $\lambda + 2G > 0$ condition of strong ellipticity is that the stiffness is positive for axial compression or extension under lateral constraint, as is the speed of longitudinal waves. Equation 3 is equivalent [8] to

$$G > 0, \qquad \frac{E(1-\nu)}{(1+\nu)(1-2\nu)} = 2G\frac{(1-\nu)}{(1-2\nu)} > 0 \tag{4}$$

in which E is Young's modulus, or

$$G > 0 \text{ and } \nu < 0.5 \text{ or } \nu > 1 \tag{5}$$

Since $E = 2G(1+\nu)$, the range of E for strong ellipticity is $-\infty < E < \infty$. As for the bulk modulus,

$$B = \frac{2G(1+\nu)}{3(1-2\nu)} \tag{6}$$

or equivalently $B = \lambda + 2G/3$, so that for strong ellipticity $-4G/3 < B < \infty$. However, as implied by Equation 1, E, G, and B must be positive for positive definiteness and for the material to be *globally* stable under small deformation.

In summary, the conditions for global stability of an elastic solid and local stability (with respect to the formation of bands) are not identical.

4.2. Nonlinear elasticity

In a one-dimensional nonlinearly elastic bar the condition for strong ellipticity is that

$$\frac{d^2W}{d\lambda^2} > 0 \tag{7}$$

in which the material in question has a strain-energy density, $W(\lambda)$, where λ is the stretch ratio (equal to $1 + \varepsilon$, with ε the engineering strain). This relation is equivalent to $d\sigma/d\lambda > 0$ with σ as the Piola (engineering) stress; that is, the stress-strain curve is monotonically increasing.

Failure of ellipticity may occur in the form of a change of sign in the slope of the stress–strain curve; the slope may become negative over an interval of strain. This was predicted [9] to result in localized deformation in the form of bands of material under high strain. Another prediction of the theory is that while the local (microscopic) stress strain curve has regions of negative slope, the macroscopic load-elongation response observed will always have a non-negative slope.

In three dimensions, the strain-energy density, $W(\lambda_1, \lambda_2, \lambda_3)$, depends nonlinearly on the three principal stretch ratios $\lambda_1, \lambda_2, \lambda_3$. The necessary and sufficient conditions of strong ellipticity (hence stability with respect to localized-strain band formation) are rather complicated [10]; see also [7] for a two-dimensional analysis. For the special case of uniaxial stress, along the λ_1 direction, the lateral stretches are equal: $\lambda_2(\lambda_1) = \lambda_3(\lambda_1)$. The three-dimensional conditions for strong ellipticity reduce to

$$\frac{\lambda_1\sigma_1}{(\lambda_1^2 - \lambda_2^2)} > 0 \tag{8}$$

$$\frac{\partial^2 W}{\partial\lambda_1^2} > 0, \qquad \frac{\partial^2 W}{\partial\lambda_2^2} > 0, \qquad \frac{\partial^2 W}{\partial\lambda_3^2} > 0 \tag{9}$$

$$\frac{\lambda_1\sigma_1}{(\lambda_1^2 - \lambda_2^2)} + \left(\frac{\partial^2 W}{\partial\lambda_1^2}\frac{\partial^2 W}{\partial\lambda_2^2}\right)^{1/2} > \left|\frac{\partial^2 W}{\partial\lambda_1\partial\lambda_2} + \frac{\lambda_2\sigma_1}{(\lambda_1^2 - \lambda_2^2)}\right| \tag{10}$$

in which $\sigma_1 = \partial W/\partial\lambda_1$ is the stress in the axial direction. We remark that Equations 9 are analogous to Equation 7 in one dimension. Experimentally, Equations 9 correspond to a condition of compression under a restriction of lateral movement as can be achieved by compression within a lubricated tube, or compression of a short block between rough platens.

5. Analysis of the experiment

The bands which develop in compressed foam are evidence of failure of ellipticity of the material viewed as a continuum. The non-monotonic, compressive-load-deformation behaviour of single-cell models is regarded as a causal mechanism for the macroscopic behaviour of the foam in the plateau region and for the banding instability.

5.1. Detailed analysis for one dimension

To understand the formation of bands, consider a one-dimensional nonlinear elastic bar with strain-energy density, $W(\lambda)$, in which λ is the stretch ratio, $\lambda = 1 + \varepsilon$ with ε the engineering strain. The stress in the bar is $\sigma = dW(\lambda)/d\lambda$. Suppose that on the continuum level, the stress strain curve (equivalent to a stress- stretch curve following a shift on the abscissa) is as shown in Fig. 4. Equilibrium requires σ = constant along the bar. It can be shown [9] that the values of the stretch in an interval $\lambda_M < \lambda < \lambda_m$ (where $d^2W/d\lambda^2 < 0$) are unstable, hence they are physically unobservable. For values of applied stress in the range $\sigma_M < \sigma < \sigma_m$ (between the local minimum and maximum of the stress–stretch curve in Fig. 4), there are two possible values of λ corresponding to the same σ, excluding the

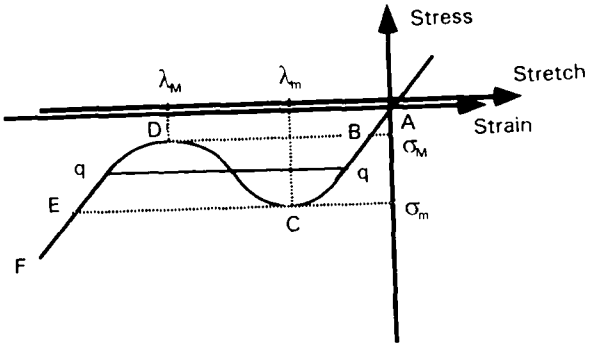

Figure 4 Schematic diagram of a non-monotonic, stress strain response. The symbols are explained in the text.

unstable middle region; these may be called λ_+ and λ_-. For values of stress outside that interval there is a unique stretch corresponding to a uniform-strain solution. In the theory of nonlinear elasticity one can model phase changes by allowing strain discontinuities while maintaining continuous displacements [7, 9, 11, 12]. In the present setting it is possible to have a discontinuity in strain. The regions of different strain (or stretch) correspond to the *bands* of localized compression observed in the experiments. The stretch is discontinuous along the bar, alternating between the values λ_+ and λ_-. The average stretch λ_{avg} must obey the relation $\lambda_- < \lambda_{avg} < \lambda_+$ so there is a constraint on the amount of material in each kind of region.

Now consider the shape of the *macroscopic* response curve. Under the above assumptions, the macroscopic response (in which stress versus average stretch is observed) is not unique but can take the form of any curve within CBDE in Fig. 4 [12]. This non-uniqueness may be removed by making additional assumptions. For example, assume that the bar undergoes deformations which minimize its total potential energy [9, 11] while satisfying the boundary conditions; then the macroscopic response exhibits a flat *plateau* region, line q–q in Fig. 4, at the Maxwell stress [9]. This stress is determined by requiring that the areas between the macroscopic and microscopic response are equal. This response is reversible, and there is no hysteresis. The macroscopic response coincides with the microscopic stress–stretch curve over the monotonically increasing portions FEq and qBA in Fig. 4. In the context of the cellular solids examined here, the theory predicts that a non-monotonic microscopic response (or a single-cell response since there is not a continuum) gives rise to a monotonically nondecreasing macroscopic response with a *plateau.*

A nonzero slope in the plateau region (such as is observed experimentally) is predicted theoretically under the assumption of inhomogeneity in the bar [11], so that the microscopic response shown in Fig. 4 differs in its details from point to point in the bar but the curve always has the same shape. In the foams this inhomogeneity is associated with small density variations throughout the foam, and variations in the buckling loads of cells depending on their geometry and orientation.

The hysteresis observed in the experiments may be explained in part by assuming an energy cost associated with movement of the edges of bands [12]. Physically, a portion of this energy dissipation can be considered to arise from the friction between cell ribs during collapse of the cells. Such analysis does not account for the hysteresis which is observed in regions other than the plateau region. A more complete analysis would incorporate the viscoelasticity of the foam material.

The width of the bands was observed to depend on the cell size. However, the classical theory of elasticity has no characteristic length scale and so cannot account for such effects. Length scales can be incorporated via Cosserat elasticity or via theories which incorporate strain gradients [13–15].

It is noteworthy that this analysis predicts a macroscopic response to be caused by a markedly different microscopic response (in a continuum sense) which corresponds to the experimentally observed behaviour of a physical single-foam-cell model.

5.2. Analysis for three dimensions

The experiments were made on three-dimensional specimens. Analysis of the three-dimensional situation is therefore called for. In the uniaxial-stress compression test of an isotropic material with a positive Poisson's ratio $\lambda_2 = \lambda_3 > \lambda_1$ and the applied compressive stress $\sigma_1 < 0$ so that Equation 10 is always true. Since the lateral surfaces in this experiment were free, $\sigma_2 = \partial W(\lambda_1, \lambda_2(\lambda_1), \lambda_3(\lambda_1))/\partial\lambda_2 = 0$, and similarly for σ_3. Differentiating with respect to λ_1

$$\frac{\partial^2 W}{\partial\lambda_1\partial\lambda_2} = -\left(\frac{\partial^2 W}{\partial\lambda_2^2} + \frac{\partial^2 W}{\partial\lambda_2\partial\lambda_3}\right)\frac{\partial\lambda_2}{\partial\lambda_1} \tag{11}$$

We also have $\sigma_1 = \partial W(\lambda_1, \lambda_2(\lambda_1), \lambda_3(\lambda_1))/\partial\lambda_1$. Differentiating with respect to λ_1

$$\frac{\partial\sigma_2(\lambda_1)}{\partial\lambda_1} = \frac{\partial^2 W}{\partial\lambda_1^2} - 2\left(\frac{\partial^2 W}{\partial\lambda_2^2} + \frac{\partial^2 W}{\partial\lambda_2\partial\lambda_3}\right)\left(\frac{\partial\lambda_2}{\partial\lambda_1}\right)^2 \tag{12}$$

We used the experimental results of Choi and Lakes [2] for Poisson's ratio versus strain to generate a plot of $\lambda_2(\lambda_1)$ against λ_1. The curve attained a relative maximum at $\lambda_1 \approx 0.85$, at which $\lambda_2 \approx 1.03$ and $\partial\lambda_2/\partial\lambda_1 = 0$. At this point in $(\lambda_1, \lambda_2, \lambda_3)$ space, assuming $\partial^2 W/\partial\lambda_2^2 > 0$ (otherwise Equation 9 fails), Equation 11 gives $\partial^2 W/\partial\lambda_1\partial\lambda_2 = 0$ and $d\sigma_1(\lambda_1)/d\lambda_1 > 0$. Then Equation 10 reduces to

$$\frac{\sigma_1}{(\lambda_1 - \lambda_2)} + \frac{d\sigma_1}{d\lambda_1}\frac{\partial^2 W}{\partial\lambda_2^2} > 0 \tag{13}$$

The first term is negative. A perfectly flat plateau corresponds to $d\sigma_1/d\lambda_1 = 0$ and therefore to failure of ellipticity. Ellipticity may also fail in the presence of a sufficiently small but positive slope in the plateau region, depending on the value of $\partial^2 W/\partial\lambda_2^2$ in contrast to the conclusions from the one-dimensional analysis; however, we do not have an experimental value for this derivative.

5.3. Discussion

Open-cell foam exhibits a monotonic stress–strain relation with a plateau region; deformation is localized in transverse bands. Single-cell models exhibit a force–deformation relation which is not monotonic. The difference between the single-cell response and the continuum response of foam is understood in terms of a stability analysis of the foam considered as an elastic continuum. A related analysis of the localization of strain in porous media has been conducted [16]. The present study, however, presents a non-monotonic force–deformation relation for the single cell as an experimentally evaluated causal mechanism for the overall foam behaviour.

6. Conclusions

1. Open-cell foam exhibits a monotonic stress–strain relation with a plateau region; deformation is localized in transverse bands of material under higher compressive strain.

2. Single-cell models exhibit a force–deformation relation which is not monotonic in compression.

3. The behaviour of the single-cell models is viewed as the cause of the banding localization and the plateau effect.

Acknowledgement

Partial support by the NASA/Boeing ATCAS program under contract # NAS1-18889, and by a University Faculty Scholar Award from the University of Iowa to R. Lakes is gratefully acknowledged. This research was conducted while R. Lakes was at the Department of Theoretical and Applied Mechanics at Cornell University. P. Rosakis wishes to acknowledge the support of the National Science Foundation through Grant # MSS-9009730.

References

1. L. J. GIBSON and M. F. ASHBY, *Cellular solids* (Pergamon, Oxford, 1988).
2. J. B. CHOI and R. S. LAKES, *J. Mater. Sci.* **28** (1993) in press.
3. W. J. STRONGE and V. P. W. SHIM, *J. Engng Mater. Technol.* **110** (1988) 185–190.
4. R. S. LAKES, *Science* **235** (1987) 1038–1040.
5. E. A. FRIIS, R. S. LAKES and J. B. PARK, *J. Mater. Sci.* **23** (1988) 4406–4414.
6. J. H. BRAMBLE and L. E. PAYNE, Proceedings of the Fourth National Congress of Applied Mechanics (1963) 469–473.
7. J. K. KNOWLES and E. STERNBERG, *J. Elasticity* **8** (1978) 329–379.
8. S. P. TIMOSHENKO and J. N. GOODIER, "Theory of elasticity", 3rd Edn (McGraw-Hill, New York, 1970).
9. J. L. ERICKSEN, *J. Elasticity* **5** (1975) 191–201.
10. H. C. SIMPSON and S. J. SPECTOR, *Arch. Rational Mech. Anal.* **84** (1983) 55–68.
11. R. D. JAMES, *ibid.* **72** (1979) 100–140.
12. R. ABEYARATNE and J. K. KNOWLES, *Int. J. Solids, Structures*, **24** (1988) 1021–1044.
13. M. E. GURTIN, in "Phase transformations and material instabilities in solids", edited by M. E. Gurtin (Academic Press, NY, 1984).
14. R. S. LAKES, *ASME J. Engng. Mater. Tech.* **113** (1990) 1313.
15. H. B. MÜHLHAUS and E. C. AIFANTIS, *Int. J. Solids Structures* in press.
16. R. ABEYARATNE and N. TRIANTAFYLLIDIS, *J. Applied Mech.* **51** (1984) 481–486.

Received 25 March 92
and accepted 15 January 1993